THE JOURNAL OF BIOLOGICAL CHEMISTRY VOL. 282, NO. 3, pp. 2091–2100, January 19, 2007

Direct Demonstration of the Flexibility of the Glycosylated Proline-Threonine Linker in the *Cellulomonas fimi* Xylanase Cex through NMR Spectroscopic Analysis*[S]

Received for publication, October 13, 2006, and in revised form, November 20, 2006 Published, JBC Papers in Press, November 22, 2006, DOI 10.1074/jbc.M609670200

David K. Y. Poon[‡§¶], **Stephen G. Withers**[‡§¶], **and Lawrence P. McIntosh**[‡§¶‖1]

From the [‡]*Department of Biochemistry and Molecular Biology,* [§]*Department of Chemistry,* [¶]*The Protein Engineering Network of Centres of Excellence, and* [‖]*The Michael Smith Laboratories, University of British Columbia, Vancouver, British Columbia V6T 1Z3, Canada*

The modular xylanase Cex (or CfXyn10A) from *Cellulomonas fimi* consists of an N-terminal catalytic domain and a C-terminal cellulose-binding domain, joined by a glycosylated proline-threonine (PT) linker. To characterize the conformation and dynamics of the Cex linker and the consequences of its modification, we have used NMR spectroscopy to study full-length Cex in its nonglycosylated (~47 kDa) and glycosylated (~51 kDa) forms. The PT linker lacks any predominant structure in either form as indicated by random coil amide chemical shifts. Furthermore, heteronuclear ^{1}H-^{15}N nuclear Overhauser effect relaxation measurements demonstrate that the linker is flexible on the ns-to-ps time scale and that glycosylation partially dampens this flexibility. The catalytic and cellulose-binding domains also exhibit identical amide chemical shifts whether in isolation or in the context of either unmodified or glycosylated full-length Cex. Therefore, there are no noncovalent interactions between the two domains of Cex or between either domain and the linker. This conclusion is supported by the distinct ^{15}N relaxation properties of the two domains, as well as their differential alignment within a magnetic field by Pf1 phage particles. These data demonstrate that the PT linker is a flexible tether, joining the structurally independent catalytic and cellulose-binding domains of Cex in an ensemble of conformations; however, more extended forms may predominate because of restrictions imparted by the alternating proline residues. This supports the postulate that the binding-domain anchors Cex to the surface of cellulose, whereas the linker provides flexibility for the catalytic domain to hydrolyze nearby hemicellulose (xylan) chains.

Cellulolytic organisms produce a battery of endo- and exoglucanases necessary for the hydrolysis of cellulose and hemicellulose. These glycoside hydrolases are typically modular, consisting of conserved catalytic and carbohydrate-binding domains (or modules), as well as possible ancillary domains, joined by variable linker sequences (1–3). In general, the constituent domains of glycoside hydrolases are structurally independent and exhibit some aspects of their respective functions when separated (4–6). Thus, binding modules appear to facilitate catalysis by targeting and maintaining the proximity of the catalytic domain toward substrates within complex macromolecular systems, such as the plant cell wall, as well as through possible disruptive effects on the structures of the polysaccharides within these systems (7, 8).

The synergistic activity of the catalytic and carbohydrate-binding domains in a glycoside hydrolase requires that they be covalently tethered to one another via a linker sequence of the appropriate length and/or flexibility. The functional importance of these interdomain linkers, which can range from only a few to over a hundred residues and are often rich in proline and hydroxyamino acids (1), has been established largely through deletion studies (9–12). However, the physical properties of glycoside hydrolase linkers remain poorly defined. The early observation that these sequences are often susceptible to proteolysis led to the hypothesis that they are exposed, flexible polypeptide regions joining independently folded catalytic and binding domains (4, 13, 14). In support of this hypothesis, initial SAXS[2] studies on cellulases from *Cellulomonas fimi* and *Humicola jecorina* indicated that these two-domain enzymes adopt an elongated tadpole shape with the head (catalytic domain) and tail (cellulose-binding domain) connected by relatively extended proline-rich and serine/threonine-rich linkers, respectively (9, 15–18). This general view has been refined through more recent SAXS analyses demonstrating that native and chimeric cellulases from *Humicola insolens* and *Pseudoalteromonas haloplanktis* adopt an ensemble of tertiary structures with a distribution of interdomain separations that is attributable to the flexibility of the intervening serine/threonine-rich

* This work was supported by grants from the Natural Sciences and Engineering Research Council of Canada with instrumentation support provided by the Protein Engineering Network of Centres of Excellence, the Canadian Foundation for Innovation, the British Columbia Knowledge Development Fund, the University of British Columbia Blusson Fund, the Michael Smith Foundation for Health Research, and the Canadian Institutes of Health Research. The costs of publication of this article were defrayed in part by the payment of page charges. This article must therefore be hereby marked "*advertisement*" in accordance with 18 U.S.C. Section 1734 solely to indicate this fact.

[S] The on-line version of this article (available at http://www.jbc.org) contains supplemental Figs. S1 and S2.

[1] To whom correspondence should be addressed: Dept. of Biochemistry and Molecular Biology, Life Sciences Centre, 2350 Health Sciences Mall, University of British Columbia, Vancouver, BC V6T 1Z3, Canada. Tel.: 604-822-3341; Fax: 604-822-5227; E-mail: mcintosh@chem.ubc.ca.

[2] The abbreviations used are: SAXS, small angle x-ray scattering; CexCD, the catalytic domain (residues 1–315) of *C. fimi* Cex; CexCBD, the cellulose-binding domain (residues 336–443) of Cex; HSQC, heteronuclear single quantum correlation; NOE, nuclear Overhauser effect; RDC, residual dipolar coupling; TROSY, transverse relaxation optimized spectroscopy; PT linker, proline-threonine linker (residues 316–335) of Cex.

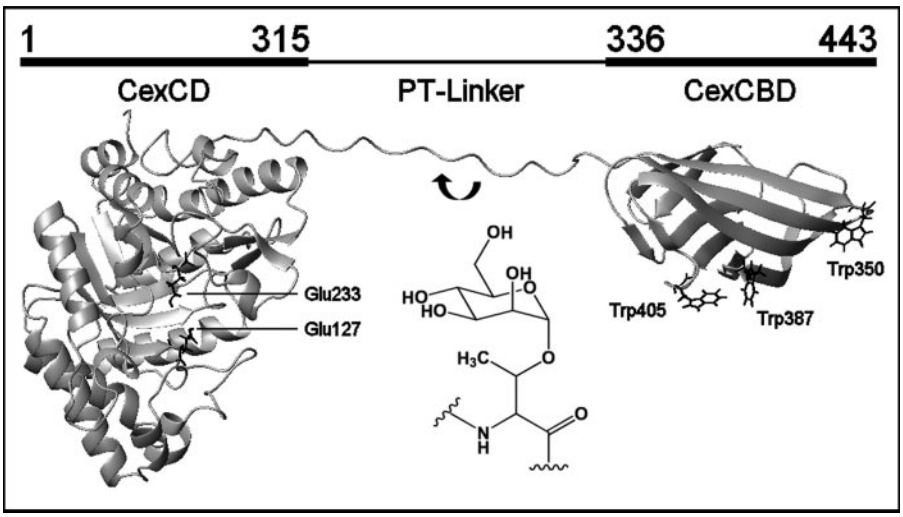

FIGURE 1. **The modular Cex consists of an N-terminal 315-residue $(\alpha/\beta)_8$-barrel catalytic domain (CexCD; Protein Data Bank code 1EX0) (26) and a C-terminal 108-residue β-barrel cellulose-binding domain (CexCBD; Protein Data Bank code 1EXG) (27), connected by a flexible proline-threonine linker (PT linker).** Also shown is the beads on a string model of Cex, illustrating the catalytic and cellulose-binding domains tethered by a conformationally flexible PT linker (drawn in an arbitrarily extended form), along with the structure of an α-D-mannopyranosylthreonine. The catalytic glutamic acid residues in the active site of CexCD and the exposed tryptophan side chains of CexCBD forming the proposed cellulose-binding surface are also identified.

linker sequences (19–21). However, because of experimental limitations, the degree of flexibility of the linker within the native *H. insolens* enzyme could not be determined directly. A comparison of the dimensions measured for various cellulases by SAXS has also led to the suggestion that glycosylation favors more extended conformations (19, 20). This conclusion is complicated by the different linker sequences of these enzymes, particularly with respect to their proline content. Regardless, such studies have led to a general model whereby some cellulases bind and cleave crystalline cellulose through a caterpillar-like motion mediated by a flexible interdomain linker (19, 20). Alternatively, in the cases of glycoside hydrolases such as the endo/exocellulase E4 from *Thermobifida fusca*, the catalytic and cellulose-binding domains are effectively fused because of the absence of a linker sequence (22). This may facilitate processivity by directing a bound cellulose strand into the active site of the enzyme.

Three-dimensional structures have also been determined by x-ray crystallography for two intact family 10 glycoside hydrolases with short linker sequences. Electron density was absent or weak for nine residues of the serine/proline-rich linker of *Streptomyces olivaceoviridis* E-26 xylanase, whereas its catalytic and carbohydrate-binding domains were found to interact directly through a hydrophilic interface (23, 24). Similarly, three linker residues were not observed between the noninteracting structured domains of *Cellvibrio japonicus* xylanase 10C (25). These studies indicated that the linkers of such family 10 enzymes are crystallographically disordered and by inference flexible but gave no direct measure of that flexibility.

To investigate on a residue-specific basis the modular structure and linker properties of a glycoside hydrolase in its unmodified and glycosylated states, we have used NMR spectroscopy to characterize the xylanase Cex (or CfXyn10A) from *C. fimi.* This model glycoside hydrolase is composed of an N-terminal family 10 catalytic domain (CexCD) (26) with highest activity for xylan hydrolysis and a C-terminal family 2 carbohydrate-binding module (CexCBD) (27), which binds preferentially to crystalline cellulose (Fig. 1), as classified by the CaZy data base (afmb.cnrs-mrs.fr/CAZY/index.html) (28, 29). These two domains are joined by a 20-residue proline-threonine linker with the sequence $(PT)_3T(PT)_3T(PT)_3$. Furthermore, this PT linker is *O*-glycosylated with α-D-mannose and α-D-galactose, such that ~24 mol of hexose are found per mole of Cex secreted by *C. fimi* (30). Early studies demonstrated that this modification leads to resistance of the Cex linker region against proteolytic degradation but that glycosylation has no significant effect upon kinetic parameters for hydrolysis of polymeric substrates (31). Without a method for the overexpression of Cex in *C. fimi*, only very small quantities of the endogenously glycosylated protein can be obtained. Fortunately, using *Streptomyces lividans*, Cex can be expressed and glycosylated in milligram amounts, as required for NMR spectroscopic characterization (30, 31). Glycosylated Cex from *S. lividans* is reported to contain ~17 mol of mannose, with traces of galactose, per mole of protein (30, 31). These differences are minor because samples of *O*-glycosylated Cex from *C. fimi* and *S. lividans* have very similar kinetic properties and are both resistant toward proteolytic degradation (31, 32). Based on chemical shift, ^{15}N relaxation, and amide residual dipolar coupling (RDC) measurements, we demonstrate that the catalytic and cellulose-binding domains are physically independent and joined by a PT linker that is conformationally dynamic on the ns-to-ps time scale. Glycosylation does not perturb either domain yet partially dampens the mobility of the linker. These data complement previous proteolysis, crystallographic, and SAXS studies, confirming directly the hypothesis that the PT linker is a flexible tether, joining the catalytic domain and cellulose-binding modules of Cex as two "beads-on-a-string."

EXPERIMENTAL PROCEDURES

Expression and Purification of Uniformly ^{15}N-labeled Cex, CexCD, and CexCBD—Nonglycosylated ^{15}N-labeled Cex, encoded by the plasmid pUC12–1.1Cex(PTIS) (33), was expressed using *Escherichia coli* BL21 (λDE3) cells grown in M9 medium enriched with 1.0 g/liter $^{15}NH_4Cl$ (Spectra Stable Isotopes Inc.). Cex and the papain-cleaved product, CexCD (residues 1–315), were expressed and purified by cellulose affinity chromatography, according to previously published protocols (34, 35). CexCBD (residues 336–443) was expressed directly using the plasmid pTug-KH_6-IEGR-CBM2a in *E. coli* BL21 (λDE3) cells (36, 37). The N-terminal His_6 tag was not removed after purification with Ni^{+2} affinity chromatography. The resulting proteins were >95% pure as judged by SDS-PAGE

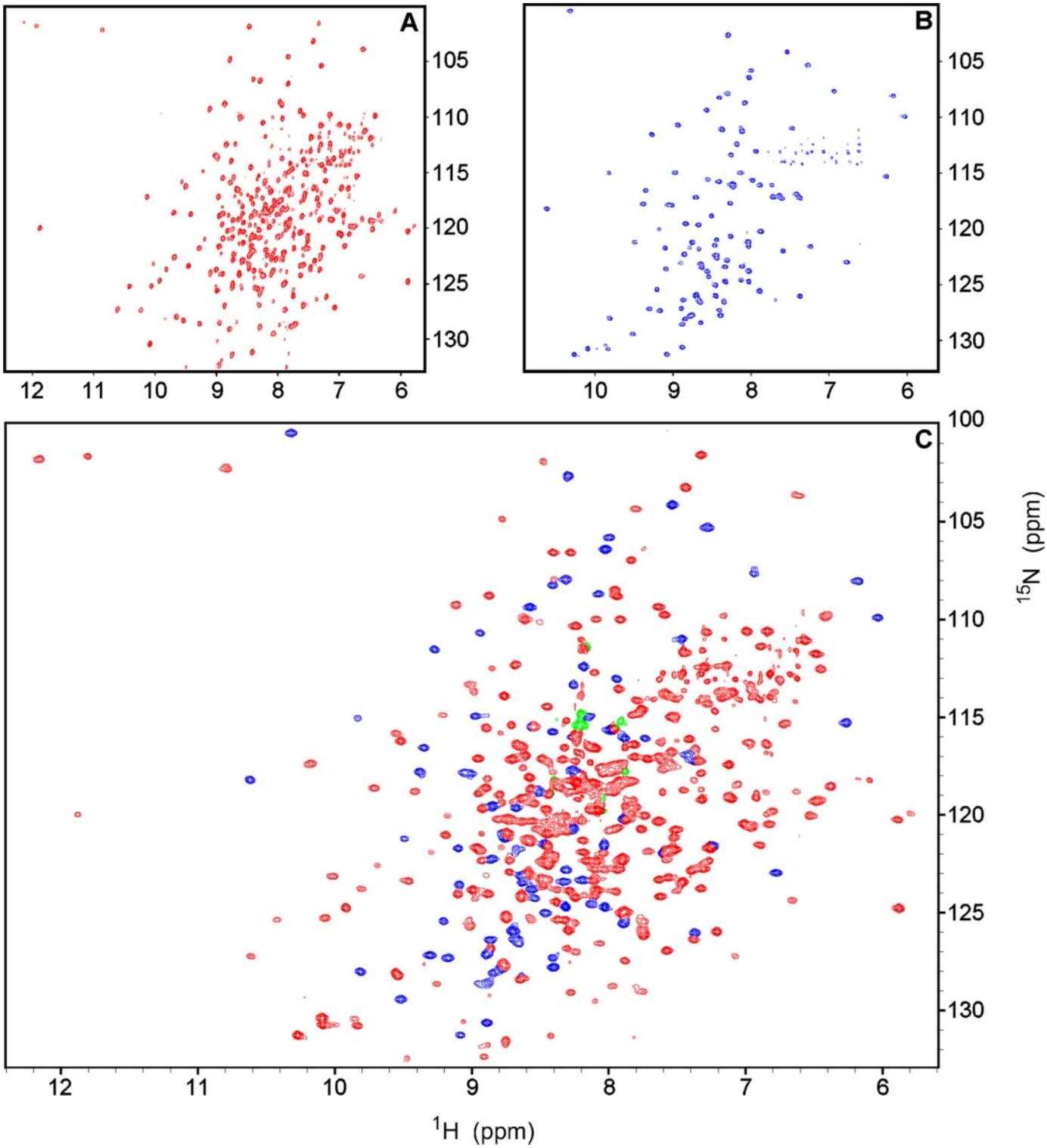

FIGURE 2. **The ^{1}H-^{15}N TROSY-HSQC spectra of uniformly ^{15}N-labeled ~0.4 mM CexCD (*A*), ~0.1 mM CexCBD (*B*), and ~0.4 mM nonglycosylated Cex (*C*), recorded at 30 °C and pH 6.5.** Signals from backbone amides and indole side chains in the catalytic domain (*red*), cellulose-binding module (*blue*), and the PT linker (*green*) were colored manually to allow a visual comparison of the spectra. The amide $^{1}H^{N}$-^{15}N assignments of Cex (not labeled for clarity) were based on those reported for the isolated CexCD (35) and CexCBD (27).

and electrospray ionization mass spectrometry (predicted for unlabeled Cex, 47,192 Da; CexCD, 34,230 Da; His_6-CexCBD, 12,272 Da). Protein concentrations were determined spectrophotometrically using predicted $\epsilon_{280\ nm}$ values of 81,440 M^{-1} cm^{-1}, 52,870 M^{-1} cm^{-1}, and 28,570 M^{-1} cm^{-1} for Cex, CexCD, and CexCBD, respectively (ExPASy website: ca.expasy.org/tools/protpar-ref.html).

Expression of ^{15}N-Thr-labeled Cex—Nonglycosylated ^{15}N-Thr-labeled Cex was produced by expression of the plasmid pUC12.1.1Cex(PTIS) in *E. coli* BL21 (λDE3) cells grown in a

synthetic medium (38) enriched with 200 mg/liter of L-threonine (^{15}N, >98%) (Cambridge Isotope Laboratory).

Expression of Glycosylated ^{15}N-Thr-labeled Cex—Glycosylated ^{15}N-Thr-labeled Cex was produced using the plasmid pIJ680-*cex* (31) in *S. lividans* 66 (TK64) cells. Transformed *S. lividans* stock (50 μl), stored in Me_2SO at −80 °C, was used to inoculate three 5-ml tryptic-soy broth cultures (EM Science), containing 20 μg/ml of thiostrepton (Sigma), in 50-ml sterile Falcon tubes. After growth in an incubator shaker at 30 °C for 48 h, the cells were collected by centrifugation, and each was used to inoculate 1.5 liters of a synthetic medium (38), containing 20 μg/ml thiostrepton, 0.016% antifoam C (Sigma), and 300 mg of L-threonine (^{15}N, >98%), in a 3-liter beveled flask. The three cultures (totaling 4.5 liters) were grown in an incubator shaker at 30 °C for 4 days, after which the *S. lividans* mycelium was removed by vacuum filtration through a Whatman glass microfiber filter. The supernatant, containing secreted glycosylated Cex, was incubated with CF-1 cellulose and purified by affinity chromatography, as described previously, yielding 37 mg of protein from 4.5 liters of isotopically enriched medium (34, 35). The purified protein was found to be heterogeneously glycosylated by SDS-PAGE and matrix-assisted laser desorption ionization-time of flight mass spectrometry analyses.

NMR Spectroscopy—NMR spectra were acquired at 30 °C on a Varian Inova 600 MHz spectrometer equipped with a gradient triple resonance cryogenic probe. All of the proteins (~0.1–0.4 mM) were in 20 mM potassium phosphate, 0.02% NaN_3 at pH 6.5 with ~10% D_2O added as a lock solvent. The spectra were processed using NMRpipe (39) and analyzed with SPARKY 3.0 (40). The main chain ^1H, ^{13}C, and ^{15}N assignments of CexCD were obtained through a suite of TROSY-based experiments, as described elsewhere (35). The $^1H^N$ and ^{15}N assignments of CexCBD were based on those reported previously (27). CexCBD weakly self-associates as revealed by concentration-dependent amide or indole chemical shift perturbations for several residues, including Trp^{350}, Trp^{387}, and Trp^{405} of the proposed cellulose-binding surface (27). Thus, ^1H-^{15}N HSQC spectra were recorded for a dilution series of CexCBD samples (~0.1–0.4 mM) to obtain concentration-independent amide chemical shifts.

$^1H^N$-^{15}N RDC values, $^1D_{NH}$, were measured from 600-MHz sensitivity-enhanced HSQC spectra of ^{15}N-labeled Cex (~0.5 mM, pH 6.5, 30 °C) in which the ^{15}N signal was recorded in the TROSY mode, whereas that of the $^1H^N$ signal was recorded in either the TROSY or anti-TROSY mode.[3] After acquiring a control spectrum, partial protein alignment was achieved by the addition of Pf1 bacteriophage (Profos AG, Regensburg, Germany) to a concentration that produced 13 Hz splitting in the ^2H NMR signal of the lock $^1HO^2H$ (41). The $^1D_{NH}$ values were obtained from the differences between the corresponding TROSY and anti-TROSY $^1H^N$ chemical shifts in the aligned *versus* control spectra of Cex. The axial (D_a) and rhombic (R) components of the alignment tensors for the residues in catalytic and cellulose-binding domains were estimated using a Matlab routine for fitting $^1D_{NH}$ distribution histograms (42), as previously described (43).

^{15}N relaxation measurements were performed using TROSY-based T_1, T_2, and heteronuclear ^1H-^{15}N NOE experiments (44, 45). Steady-state heteronuclear ^1H-^{15}N NOE values were measured by recording spectra with and without 3 s of proton saturation and a total recycle delay of 5.016 s. Analysis of the ^{15}N relaxation data were carried out using SPARKY 3.0 (40) and TENSOR2 (46).

[3] L. E. Kay, personal communication.

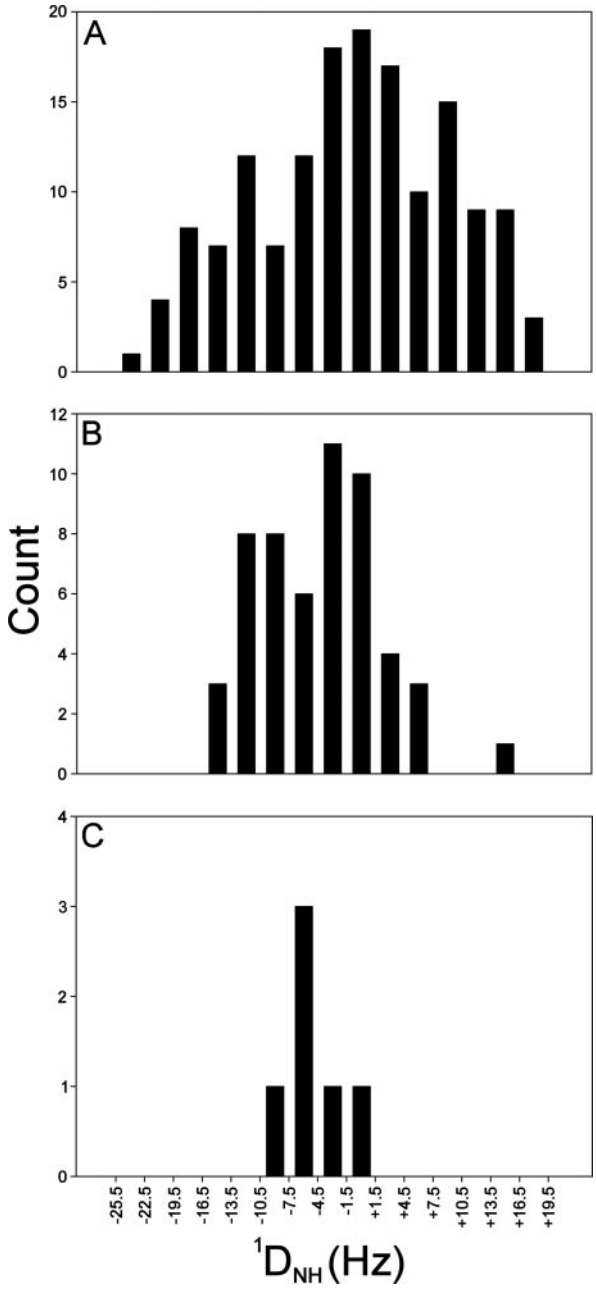

FIGURE 3. **Interdomain mobility in Cex is confirmed by $^1D_{NH}$ RDCs measured for amides in the catalytic domain (*A*), cellulose-binding domain (*B*), and PT linker (*C*) of the full-length enzyme.** The different maximum, minimum, and most frequent values of these distributions reveal that the two domains and the PT linker have distinct alignment tensors describing their different average orientations with respect to the magnetic field because of weak interactions with Pf1 phage (42, 48).

RESULTS

NMR Spectral Comparisons Confirm That the Catalytic and Cellulose-binding Domains of Cex Are Structurally Independent—The ^1H-^{15}N TROSY-HSQC spectrum of non-glycosylated full-length Cex is presented in Fig. 2*C*. The

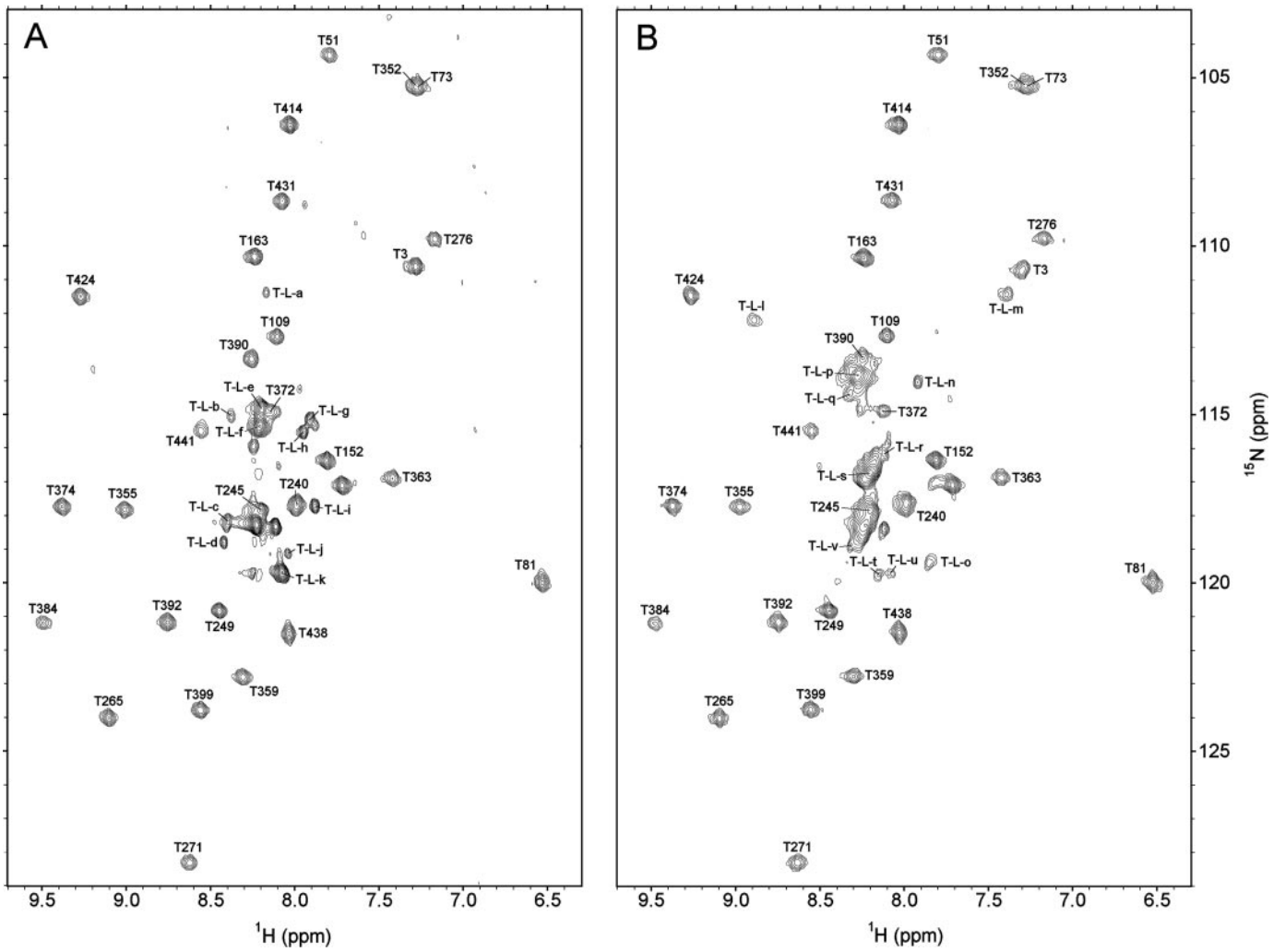

FIGURE 4. **The ^{1}H-^{15}N TROSY-HSQC spectra of selectively ^{15}N-Thr-labeled Cex in its nonglycosylated (*A*) and glycosylated (*B*) forms reveal that the PT linker is unstructured and that glycosylation does not induce any predominant structure.** The well dispersed signals are assigned to threonine amides within the catalytic and cellulose-binding domains, based on comparisons to the spectra of CexCD and CexCBD. The remaining peaks, with random coil $^{1}H^{N}$ chemical shifts, correspond to threonine residues in the nonglycosylated and glycosylated PT linker. These peaks were not specifically assigned and are identified alphabetically with the prefix *T-L*. Additional weak signals are attributed to *cis-trans*-isomerization of the Thr-Pro amides (*A* and *B*), along with heterogeneous glycosylation (*B*).

remarkably well dispersed spectrum of this 443 residue (~47 kDa) protein overlaps almost exactly with the sum of the spectra of the isolated CexCD and CexCBD (Fig. 2, *A* and *B*). Assuming that peaks with the closest $^{1}H^{N}$ and ^{15}N chemical shifts in the overlapped spectra of the three species correspond to the same residue, we were able to comparatively assign the amide resonances from the catalytic and cellulose-binding domains of Cex based on the reported assignments of its isolated constituent domains (27, 35). The remaining signals in the TROSY-HSQC spectrum of Cex, all of which fall within the crowded region of ~7.9–8.4 ppm in the ^{1}H dimension, were attributed to linker threonines, as discussed below.

The $^{1}H^{N}$ and ^{15}N chemical shifts of an amide are strongly dependent upon its environment within a protein, and thus shift perturbations provide a very sensitive measure of potential structural interactions. The lack of any significant chemical shift differences between corresponding amides in the respective isolated catalytic and cellulose-binding domains and those in the full-length protein (quantitatively shown in supplemental Fig. S1) strongly indicates that the two modules of Cex do not interact noncovalently when tethered by the PT linker, nor are they perturbed by the presence of the linker. To confirm this conclusion, ^{1}H-^{15}N TROSY-HSQC spectra of full-length Cex were also recorded under identical conditions before and after treatment with papain to cleave the PT linker *in situ*. Without exception, the resolved resonances observed from residues of the catalytic and cellulose-binding module retained the same chemical shifts before and after proteolysis (data not shown).

^{15}N Relaxation and RDC Measurements Reveal the Interdomain Mobility of Cex—The global dynamic properties of intact Cex were compared with those of CexCD and CexCBD using ^{15}N relaxation measurements. Based on amide ^{15}N T_1 and T_2 values, the effective correlation times (τ_c) for the tumbling of the catalytic and cellulose-binding domains in full-length Cex (0.4 mM) were determined to be 17.6 ± 1.1 and 14.3 ± 1.0 ns, respectively. As expected because of their physical linkage, these values are higher than those measured for the isolated 34-kDa CexCD (16.1 ± 0.1 ns; ~0.4 mM) and 12-kDa CexCBD

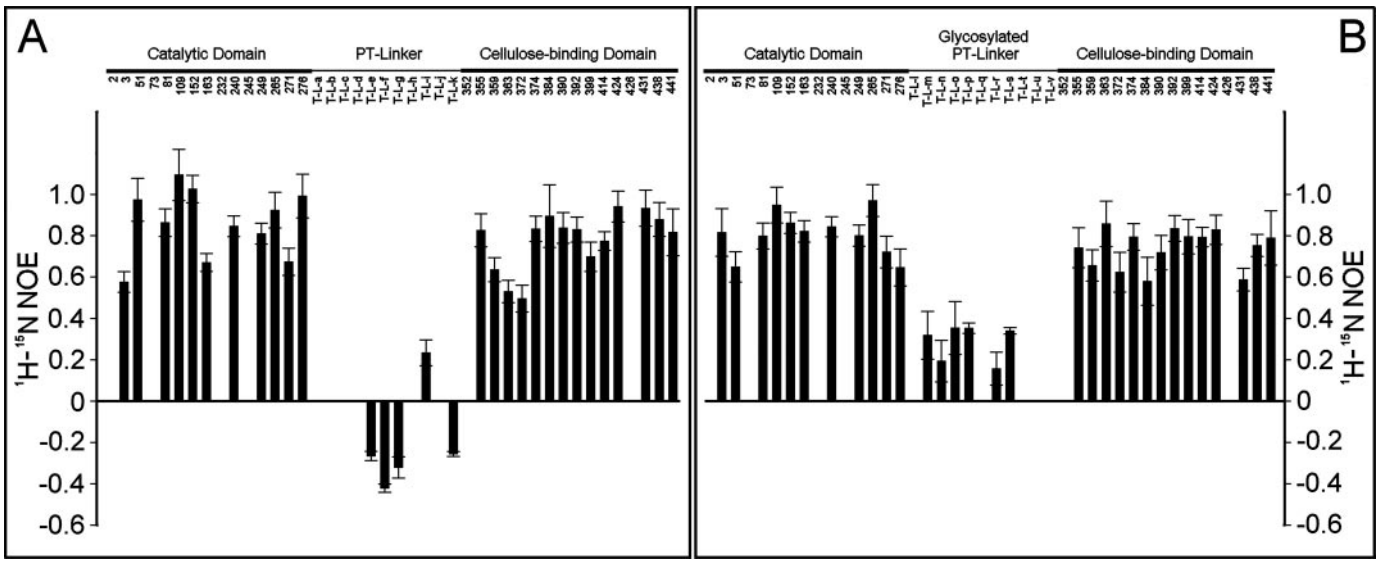

FIGURE 5. **Heteronuclear ^{1}H-^{15}N NOE measurements of selectively ^{15}N-Thr-labeled Cex in its nonglycosylated (*A*) and glycosylated (*B*) forms reveal that the PT linker is conformationally mobile on the ns-ps time scale and that glycosylation partially dampens this mobility.** Decreasing heteronuclear ^{1}H-^{15}N NOE values indicate increasing mobility on this time scale. In contrast to the threonines from the structured catalytic and cellulose-binding domains, those from the PT linker were not specifically assigned and thus are alphabetically labeled (see Fig. 4), without any implied correlation between corresponding residues in the two forms of Cex. Missing data points correspond to threonines that are unassigned and/or poorly resolved.

(8.4 ± 0.1 ns; ~0.1 mM). Also, whereas the anisotropic diffusion tensor of CexCD (with D_{zz}:D_{yy}:D_{xx} equal to 1.26:1.03:1.00) is consistent with its crystallographically determined prolate ellipsoid shape (35), that of the corresponding catalytic domain in Cex (2.1:1.6:1.0) is distinctly anisotropic because of the attached linker and cellulose-binding domain. Similarly, the diffusion tensor of the cellulose-binding domain of Cex differs from that of CexCBD because of the attached linker and catalytic domain (not shown). Most importantly, however, the observation that the effective τ_c values of the two domains within Cex differ significantly from one another and from that of ~25 ns predicted for a globular 47-kDa protein (47) indicates that they tumble semi-independently while tethered to one another by the PT linker.

Additional evidence for the structural and dynamic independence of the catalytic and cellulose-binding domains within native Cex is provided by amide $^1D_{NH}$ RDC measurements. RDCs, which arise upon the weak alignment of a macromolecule in a magnetic field, provide information on long range orientations. In the case of a multi-domain protein with minimal interdomain mobility, the average orientation of each domain will be described by a single, common molecular alignment tensor. In contrast, if medium to large scale interdomain motions occur, then the average orientations of the domains may differ because of different weak interactions with the alignment medium, thereby leading to distinct alignment tensors (48). Using TROSY-based HSQC experiments, we measured $^1D_{NH}$ values for 151 and 54 amides belonging to the catalytic and cellulose-binding domains, respectively, in full-length Cex. Inspection of the histograms showing the resultant $^1D_{NH}$ RDC distributions (Fig. 3) reveals that the two domains indeed have distinct alignment tensors. This conclusion is confirmed quantitatively by fitting of the histograms (43) to yield values of −10 Hz and 0.6 for the axial (D_a) and rhombic (R) components of the alignment tensor for the catalytic domain, respectively, as compared with +9 Hz and 0.4 for the cellulose-binding domain. Thus, the two domains within Cex are oriented at least semi-independently by differential steric and electrostatic interactions with Pf1 phage (49) rather than behaving as a single rigid body.

PT Linker of Nonglycosylated Cex Is Unstructured and Conformationally Dynamic—In addition to signals from its catalytic domain and cellulose-binding module, the ^{1}H-^{15}N TROSY-HSQC spectrum of uniformly ^{15}N-labeled Cex contains several peaks, clustered near 7.9–8.4 ppm in the ^{1}H dimension, that likely arise from the threonine amides within the PT linker. The ^{1}H-^{15}N TROSY-HSQC spectrum of Cex, selectively labeled with ^{15}N-Thr, was recorded to help resolve and identify these signals (Fig. 4*A*). This simplified spectrum contains a set of well dispersed signals, combined with a group of sharp, overlapping peaks. Based on the reported assignments of CexCD and CexCBD, the former signals can be readily assigned to threonines within the structured catalytic and cellulose-binding domains. Thus, the remaining identifiable peaks must arise from the 11 threonines in the PT linker. Because of their spectral overlap, as well as the repetitive nature of the linker sequence, it was not possible to assign these signals to specific residues without additional approaches, such as the preparation of an expensive ^{13}C/^{15}N-Pro- and -Thr-labeled protein sample (50). Nevertheless, it is readily apparent that all of the linker threonines have poorly dispersed amide $^1H^N$ chemical shifts within the range expected for a random coil polypeptide (51). (A distribution of ~4 ppm in ^{15}N chemical shift is expected because of nearest neighbor threonine and proline effects (51).) This indicates either that the PT linker lacks any predominant structure or that the repetitive linker sequence led to a repetitive structure, which does not result in the dispersion of the threonine amide chemical shifts. Based on relaxation measurements, as discussed below, the former conclusion is strongly favored. In addition, close inspection of the

^{1}H-^{15}N TROSY-HSQC spectrum of ^{15}N-Thr-labeled Cex reveals the presence of several weak peaks within this narrow chemical shift range. These most likely reflect conformational heterogeneity of the unstructured linker caused by *cis-trans* isomerization of the Thr-Pro peptide bonds.

To directly probe the dynamic properties of the nonglycosylated PT linker, steady-state heteronuclear ^{1}H-^{15}N NOE measurements were also carried out with selectively ^{15}N-Thr-labeled Cex. The heteronuclear NOE is a sensitive indicator of a sub-ns time scale dynamics, with decreasing values corresponding to increasing mobility of the amide $^{1}H^{N}$-^{15}N bond vector (52). As shown in Fig. 5*A*, threonine amides within the catalytic and cellulose-binding domains have uniformly high heteronuclear NOE values, consistent with their well structured environments. In marked contrast, those from the PT linker exhibit low or negative heteronuclear NOE values, clearly demonstrating that they are conformationally flexible on the ns-to-ps time scale. As a further reflection of this flexibility, five linker threonines with resolved signals in the ^{15}N T_1, T_2, and heteronuclear NOE relaxation spectra recorded for uniformly ^{15}N-labeled Cex, were fit to model-free order parameters, S^2, of ~0.45 (and an effective τ_c of ~6 ns), whereas amides in the catalytic and cellulose-binding domains had S^2 values of ~0.9 (35, 53). This generalized Lipari-Szabo order parameter decreases from 1 to 0 with decreasing spatial restriction of the NH bond vector. It is also noteworthy that PT linker threonines with resolved signals in the spectrum of uniformly ^{15}N-labeled Cex yielded relatively small amide $^{1}D_{NH}$ RDC values ranging from −8 to 0 Hz (Fig. 3*C*). Although this could be due to well oriented $^{1}H^{N}$-^{15}N bond vectors at angles with respect to the magnetic field that simply produce small dipolar couplings, in combination with relaxation measurements, a more likely explanation is that the net orientation of the PT linker in Cex aligned by Pf1 phage is small because of its conformational mobility.

Production of Glycosylated Cex—To examine the effects of glycosylation on the structure and dynamics of Cex, *S. lividans* was used as a surrogate expression host. Unfortunately, we were unable to prepare a uniformly ^{15}N-labeled sample of glycosylated Cex because of poor protein expression by this bacterium grown in M9 minimal medium. However, using a synthetic medium supplemented with ^{15}N-threonine (38), dispersed mycelial growth of *S. lividans* was achieved, leading to the production of glycosylated ^{15}N-Thr-labeled Cex. Based on matrix-assisted laser desorption ionization-time of flight mass spectrometry, the expressed Cex was heterogeneously glycosylated, with an average molecular mass of 51,173 Da (range, ~48–53 kDa), corresponding to an average of ~25 hexose residues/protein molecule.

PT Linker Glycosylation Does Not Perturb the Catalytic or Cellulose-binding Domains—The ^{1}H-^{15}N TROSY-HSQC spectrum of glycosylated ^{15}N-Thr-labeled Cex is shown in Fig. 4*B*. Similar to that of the nonglycosylated protein, this spectrum consists of a set of well dispersed peaks, assignable to the catalytic and cellulose-binding domains. A comparison of the $^{1}H^{N}$ and ^{15}N chemical shifts of the threonines within these domains in the absence and presence of glycosylation revealed no significant spectral perturbations (supplemental Fig. S2). Only Thr^{3} showed a minor shift difference (~0.02 ppm), and this can be attributed to its spatial proximity to the C terminus of the catalytic domain and hence to the glycosylated linker. Overall, the lack of any significant chemical shift perturbations demonstrates that glycosylation of Cex does not alter the structural environments of the threonines within either domain in the full-length protein. This also confirms previous studies demonstrating that glycosylation occurs exclusively within the PT linker and not in the structured domains of Cex (30). Furthermore, based on ^{15}N T_1 and T_2 relaxation measurements for 11 and 13 threonines, the effective τ_c values for the catalytic and cellulose-binding domains in glycosylated ^{15}N-Thr-labeled Cex (0.4 mM) were determined to be 21.3 ± 1.1 and 18.3 ± 0.6 ns, respectively. As expected, these values are higher than those measured for the unmodified protein because of the increased average molecular mass of ~4 kDa from the added sugars, possibly combined with reduced linker flexibility (discussed below). However, the fact that the two domains exhibit significantly different diffusion properties indicates that they still tumble semi-independently while tethered by the glycosylated PT linker.

PT Linker of Glycosylated Cex Remains Predominantly Unstructured and Conformationally Dynamic—After accounting for the threonines in the catalytic and cellulose-binding domains, the remaining peaks in the ^{1}H-^{15}N TROSY-HSQC spectrum of ^{15}N-Thr-labeled Cex from *S. lividans* must arise from the glycosylated PT linker. These include a cluster of strong signals with random coil $^{1}H^{N}$ chemical shifts. Several weak signals, including two peaks with amide shifts outside of the random coil range (labeled *T-L-l* and *-m* in Fig. 4*B*) are also detected, indicative of heterogeneous glycosylation and/or *cis-trans* Thr-Pro isomerization. Because of this post-translational modification, the chemical shifts of the linker threonines differ in the HSQC spectra of glycosylated *versus* nonglycosylated Cex. Along with the lack of specific assignments, this precluded a residue-by-residue comparison of the interdomain sequence in the two forms of Cex. Nevertheless, the observation of random coil chemical shifts demonstrates that the PT linker remains predominantly unstructured upon glycosylation. The more dispersed $^{1}H^{N}$ chemical shifts of two of the threonines may reflect local conformational effects caused by the attached hexose moieties.

The dynamic properties of glycosylated ^{15}N-Thr-labeled Cex were also investigated by ^{15}N relaxation measurements (Fig. 5*B*). Similar to the nonglycosylated form of the protein, threonines within the well structured catalytic and cellulose-binding domains exhibited uniformly high ^{1}H-^{15}N NOE values. In contrast, PT linker threonines showed reduced ^{1}H-^{15}N NOE values, indicative of significantly greater flexibility on the sub-ns time scale. However, these values were consistently positive and higher than those observed with unmodified Cex (Fig. 5*A*). Furthermore, fitting of the relaxation data measured for four linker threonines with strong, resolved signals yielded an average effective τ_c of ~8 ns and an average S^2 of ~0.8. Although complicated by heterogeneous levels of modification, these values are clearly higher than those found for unmodified Cex, thus demonstrating that glycosylation partially dampens the fast time scale mobility of the PT linker.

DISCUSSION

Cex Is Composed of Independent Catalytic and Cellulose-binding Domains Tethered by a Flexible PT Linker—We have used NMR spectroscopy to characterize native Cex in its non-glycosylated and glycosylated forms. In particular, this represents the first direct conformational study of the PT linker from such a class of modular glycoside hydrolases. Although Cex is a ~47-kDa protein, it yields excellent quality NMR spectra, likely because of the independence of its well folded constituent domains. Based on amide chemical shift comparisons, combined with amide RDC and ^{15}N relaxation measurements, we demonstrate that the catalytic domain and cellulose-binding domain in Cex behave as beads-on-a-string joined by a flexible linker (Fig. 1). This conclusion is supported by several lines of evidence. First, the lack of any significant chemical shift differences between corresponding amides in full-length Cex *versus* isolated CexCD or CexCBD (separated or mixed) reveals that the catalytic and cellulose-binding domains do not interact detectably in a noncovalent manner with one another, or with the PT linker, when tethered together in their native context. Second, the significantly different effective τ_c values (17.6 ± 1.1 ns *versus* 14.3 ± 1.0 ns) measured for the two domains in Cex indicate that each undergoes rotational diffusion semi-independently. Third, the interdomain mobility of Cex is also reflected by the distinct alignment tensors describing the differential orientation of its constituent catalytic and cellulose-binding domains by Pf1 phage. Fourth, in contrast to these well structured domains, the threonine residues within the PT linker have random coil chemical shifts, low or negative heteronuclear ^{1}H-^{15}N NOE values, and small $^{1}D_{NH}$ RDC values. Thus, this segment of Cex is predominantly unstructured and conformationally mobile on the ns-ps time scale.

Not unexpectedly, the structural organization of Cex is consistent with the functional properties of this well characterized glycoside hydrolase. In particular, the enzymatic activity of isolated CexCD toward cleavage of soluble substrates is similar to that of the full-length Cex, with or without linker glycosylation (32, 54). Thus, neither the linker nor the cellulose-binding module alters the catalytic properties of the catalytic domain of Cex. Likewise, the relative binding affinities of nonglycosylated Cex and the isolated CexCBD for microcrystalline cellulose (Avicel) are very similar, indicating that the catalytic domain and linker neither contribute to, nor interfere with, cellulose binding (55). Complementing these findings, thermal denaturation studies also revealed that the stabilities of the catalytic domain and cellulose-binding modules of Cex do not change significantly upon their separation (56).

Glycosylation Partially Dampens the Fast Time Scale Motions of the PT Linker but Does Not Perturb the Catalytic or Cellulose-binding Domains—The effects of glycosylation on Cex were investigated using selectively ^{15}N-Thr-labeled protein produced in *S. lividans*. To the best of our knowledge, this represents the first time that a prokaryotic expression host has been used to overexpress a glycosylated isotopically labeled protein for NMR spectroscopic analyses. Based on their invariant threonine $^{1}H^{N}$ and ^{15}N chemical shifts, glycosylation of the PT linker does not affect the structure of either the catalytic or cellulose-binding domains of Cex. This is consistent with the similar catalytic activities of unmodified and glycosylated Cex toward soluble substrates (20, 22). Furthermore, glycosylation does not induce any predominant structure in the PT linker, as shown by the random coil shifts of its constituent threonines. The glycosylated PT linker also remains flexible on the sub-ns time scale, as indicated by ^{1}H-^{15}N NOE values significantly lower than those measured for the threonines in the structured catalytic and binding domains.

The fast time scale dynamics of the glycosylated PT linker are, however, dampened relative to the unmodified linker, as reflected by slower effective τ_c and increased ^{1}H-^{15}N NOE and S^2 values compared with the unmodified linker. These observed dynamic changes, which should be viewed qualitatively because of heterogeneous levels of glycosylation, may result from increased hydrodynamic drag from the covalently attached α-mannose residues and/or steric interactions restricting the conformational space accessible to the PT linker. Indeed, light scattering and ^{13}C NMR spectroscopic studies have demonstrated that extensive *O*-glycosylation leads to a pronounced lengthening and stiffening of the polypeptide chain of ovine submaxillary mucin (57, 58). Likewise, SAXS analysis suggested that the glycosylated "double linker" in a chimeric cellulase was significantly longer than expected for a random coil, leading to the hypothesis that steric restraints introduced by the attached sugars drive its conformational ensemble toward more extended forms (20).

The restricted flexibility of the PT linker upon *O*-glycosylation may in turn reduce the relative mobility and increase the average separation of the catalytic and cellulose-binding domains of Cex. Along with an overall increase of ~4 kDa in mass, this may lead to the slower effective τ_c values measured for the two domains relative to their counterparts in the unmodified protein. However, it remains to be established whether or not this alters the activity of Cex toward its natural substrates. To date, the best documented role of glycosylation is to enhance the viability of Cex in an extracellular environment by providing protection for the proteolytically vulnerable PT linker (31). In addition, the presence of glycans has been reported to marginally increase the relative affinity of a Cex fragment, comprising only of the PT linker plus CexCBD, relative to its nonglycosylated counterpart for crystalline cellulose, possibly through direct sugar-sugar interactions (30).

Implications for the Structure of Cex—The demonstration by NMR methods that Cex is composed of independent, well folded catalytic and cellulose-binding domains tethered by a flexible PT linker refines the structural model for this glycoside hydrolase. From early SAXS measurements, the maximum dimension of Cex within its conformational ensemble that contributes detectably to scattering, D_{max}, was reported to be ~140 Å (18). With consideration of the known structures of CexCD and CexCBD, this corresponds to a D_{max} for the 20 residue PT linker of ~50–70 Å. This value is similar to that of ~65 Å estimated for the highly related 23 residue PT linker of CenA from a comparison of D_{max} values measured for the wild type and a deletion mutant of this *C. fimi* endoglucanase (9). The average D_{max} of ~3 Å/residue for these PT linkers corresponds to a relatively extended conformation. Neighboring Cα-to-Cα

distances for α-helices and β-strands are 1.5 and 3.3 Å, respectively (59), and a statistical analysis of helical and extended linkers yielded average displacements of 1.5 and 3 Å/residue, respectively (60). The central proline tripeptide observed with weak electron density in the linker of *S. olivaceoviridis* E-26 xylanase spans a Cα-to-Cα distance of 3.3 Å/residue (24).

The PT linkers of Cex and CenA were initially described as extended and rigid because of the relatively large D_{max} values measured by SAXS (9). However, as discussed above, NMR spectroscopy reveals that the linker of Cex is predominantly unstructured and flexible on the ns-ps time scale. In this respect, the two techniques are complementary because SAXS provides a measure of the possible extension of a molecule but only indirect insights into its motional properties, whereas NMR spectroscopy most readily yields local dynamic rather than global structural information. Based on chemical shift, ^{15}N relaxation, and RDC measurements, the fast dynamics of the PT linker likely arise from local backbone mobility; however, concerted motions of segments of the linker may also occur. NMR studies have indicated that proline/alanine-rich peptides, corresponding to sequences in the light chain of skeletal myosin and in the pyruvate dehydrogenase complex, are not simple random coils but rather preferentially adopt extended conformations with partially restricted flexibility (61, 62). With a cyclized side chain, prolines disfavor α-helices because of their inability to act as hydrogen bond donors, combined with steric interactions of their $C^{\delta}H_2$ group that bias the ψ dihedral angle of the preceding residue to the β-sheet region ($\psi \sim +135°$) of the Ramachandran plot. At the same time, with a φ dihedral angle constrained near −65°, prolines cannot adopt an antiparallel β-strand conformation ($\phi \sim -140°$) (63). Thus, we propose that Cex adopts an ensemble of linker conformations to yield a distribution of orientations and spacings between its catalytic and cellulose-binding domains; however, more extended structures likely predominate because of backbone conformational restrictions imparted by the alternating proline residues. Glycosylation may further bias this distribution toward elongated states.

It is instructive to compare the properties of the *C. fimi* PT linkers with those reported for the glycosylated serine/threonine-rich linkers in *H. insolens* Cel45 (36 residues) and a chimera constructed from Cel6A and Cel6B of this saprophytic fungus (88 residues) (19, 20). Significantly shorter displacements of ~1.4 and ~0.7 Å/residue were estimated from the SAXS-determined D_{max} values of these linkers. Furthermore, detailed fitting of the scattering profile of Cel6A/B revealed that the chimera adopts an ensemble of structures with varying interdomain spacings and that the flexible linker adopts a nonrandom distribution of conformations, with a preference for more compact states. Such compact states may be less favored with PT linkers because of their higher content of proline residues.

Implications for Catalysis by Cex—Consistent with previous enzymatic, ligand binding, and thermal denaturation studies, our current NMR spectroscopic analyses demonstrate that Cex is composed of structurally independent catalytic and cellulose-binding domains, tethered by a flexible proline-threonine linker. This model, summarized in Fig. 1, supports the hypothesis that the cellulose-binding domain targets Cex to crystalline regions of cellulose within the plant cell wall (54, 64) and thereby enhances the activity of the catalytic domain by maintaining its local concentration and prolonged association with nearby hemicellulose (xylan) chains (12). Simple modeling suggests that the distance between the active site of Cex and the edge of its cellulose-binding domain can range from ~20 to 80 Å as the end-to-end distance of the flexible PT linker increases. This would correspond to ~6 xylobiose units that could be cleaved by a caterpillar-like motion of Cex with its cellulose-binding domain anchored at a fixed position. Possible preferences of the PT linker for extended conformations, particularly when glycosylated, may restrict this range. The ability of the binding domain to diffuse along the surface of cellulose (65) would then allow the progressive hydrolysis of more distant hemicellulose chains. The cellulose-binding domain may also contribute by disrupting weakly order regions of the cellulose fibers (66).

In conclusion, this study definitively demonstrates that PT linkers of the type found in Cex are flexible, albeit less so in their glycosylated state. These results complement recent SAXS studies on cellulases with linkers of a lower proline content, which demonstrate an ensemble of interdomain spacings and thus imply that the linker is flexible (19–21). Together, these data support a model of modular cellulase/hemicellulase action in which the cellulose-binding domain serves as an anchor point on the plant cell wall, whereas the catalytic domain performs polymer hydrolysis via a caterpillar-like motion that is coupled with diffusion of the binding domain on the cellulose surface. A linker sequence of the appropriate length and/or flexibility is clearly crucial to this mode of action.

Acknowledgments—We thank Tony Warren, Bernard Henrissat, and the anonymous reviewers for valuable comments; Emily Kwan and Doug Kilburn for advice on protein expression; Lewis Kay, Ranjith Muhandiram, Gregory Lee, and Mark Okon for assistance with NMR spectroscopy; James Choy and Nikolai Skrynnikov for providing MatLab RDC analysis routines; and Gary Yalloway and Shouming He for mass spectrometric analyses within the University of British Columbia Proteomics Core Facility.

REFERENCES

1. Gilkes, N. R., Henrissat, B., Kilburn, D. G., Miller, R. C., Jr., and Warren, R. A. (1991) *Microbiol. Rev.* **55,** 303–315
2. Gilbert, H. J., and Hazlewood, G. P. (1993) *J. Gen. Microbiol.* **139,** 187–194
3. Beguin, P., and Aubert, J. P. (1994) *FEMS Microbiol. Rev.* **13,** 25–58
4. Tomme, P., Vantilbeurgh, H., Pettersson, G., Vandamme, J., Vandekerckhove, J., Knowles, J., Teeri, T., and Claeyssens, M. (1988) *Eur. J. Biochem.* **170,** 575–581
5. Coutinho, J. B., Gilkes, N. R., Kilburn, D. G., Warren, R. A. J., and Miller, R. C. (1993) *FEMS Microbiol. Lett.* **113,** 211–218
6. Hall, J., Black, G. W., Ferreira, L. M. A., Millwardsadler, S. J., Ali, B. R. S., Hazlewood, G. P., and Gilbert, H. J. (1995) *Biochem. J.* **309,** 749–756
7. Boraston, A. B., Bolam, D. N., Gilbert, H. J., and Davies, G. J. (2004) *Biochem. J.* **382,** 769–781
8. Shoseyov, O., Shani, Z., and Levy, I. (2006) *Microbiol. Mol. Biol. Rev.* **70,** 283–295
9. Shen, H., Schmuck, M., Pilz, I., Gilkes, N. R., Kilburn, D. G., Miller, R. C., and Warren, R. A. J. (1991) *J. Biol. Chem.* **266,** 11335–11340
10. Srisodsuk, M., Reinikainen, T., Penttila, M., and Teeri, T. T. (1993) *J. Biol. Chem.* **268,** 20756–20761

11. Black, G. W., Rixon, J. E., Clarke, J. H., Hazlewood, G. P., Theodorou, M. K., Morris, P., and Gilbert, H. J. (1996) *Biochem. J.* **319,** 515–520
12. Black, G. W., Rixon, J. E., Clarke, J. H., Hazlewood, G. P., Ferreira, L. M. A., Bolam, D. N., and Gilbert, H. J. (1997) *J. Biotechnol.* **57,** 59–69
13. van Tilbeurgh, H., Tomme, P., Claeyssens, M., Bhikhabhai, R., and Pettersson, G. (1986) *FEBS Lett.* **204,** 223–227
14. Gilkes, N. R., Warren, R. A., Miller, R. C., Jr., and Kilburn, D. G. (1988) *J. Biol. Chem.* **263,** 10401–10407
15. Abuja, P. M., Pilz, I., Claeyssens, M., and Tomme, P. (1988) *Biochem. Biophys. Res. Commun.* **156,** 180–185
16. Abuja, P. M., Schmuck, M., Pilz, I., Tomme, P., Claeyssens, M., and Esterbauer, H. (1988) *Eur. Biophys. J. Biophys. Lett.* **15,** 339–342
17. Pilz, I., Schwarz, E., Kilburn, D. G., Miller, R. C., Jr., Warren, R. A., and Gilkes, N. R. (1990) *Biochem. J.* **271,** 277–280
18. Miller, R., Jr., Gilkes, N., Johnson, P., Kilburn, D., Kwan, E., Meinke, A., Schmuck, M., Hua, S., Tomme, P., and Warren, A. (1995) in *Proceedings of Sixth International Conference on Biotechnology in the Pulp and Paper Industry*, June 11–15, 1995, Vienna, Austria
19. Receveur, V., Czjzek, M., Schulein, M., Panine, P., and Henrissat, B. (2002) *J. Biol. Chem.* **277,** 40887–40892
20. von Ossowski, I., Eaton, J. T., Czjzek, M., Perkins, S. J., Frandsen, T. P., Schulein, M., Panine, P., Henrissat, B., and Receveur-Brechot, V. (2005) *Biophys. J.* **88,** 2823–2832
21. Violot, S., Aghajari, N., Czjzek, M., Feller, G., Sonan, G. K., Gouet, P., Gerday, C., Haser, R., and Receveur-Brechot, V. (2005) *J. Mol. Biol.* **348,** 1211–1224
22. Sakon, J., Irwin, D., Wilson, D. B., and Karplus, P. A. (1997) *Nat. Struct. Biol.* **4,** 810–818
23. Fujimoto, Z., Kuno, A., Kaneko, S., Yoshida, S., Kobayashi, H., Kusakabe, I., and Mizuno, H. (2000) *J. Mol. Biol.* **300,** 575–585
24. Fujimoto, Z., Kuno, A., Kaneko, S., Kobayashi, H., Kusakabe, I., and Mizuno, H. (2002) *J. Mol. Biol.* **316,** 65–78
25. Pell, G., Szabo, L., Charnock, S. J., Xie, H., Gloster, T. M., Davies, G. J., and Gilbert, H. J. (2004) *J. Biol. Chem.* **279,** 11777–11788
26. White, A., Withers, S. G., Gilkes, N. R., and Rose, D. R. (1994) *Biochemistry* **33,** 12546–12552
27. Xu, G. Y., Ong, E., Gilkes, N. R., Kilburn, D. G., Muhandiram, D. R., Harrisbrandts, M., Carver, J. P., Kay, L. E., and Harvey, T. S. (1995) *Biochemistry* **34,** 6993–7009
28. Henrissat, B., and Davies, G. (1997) *Curr. Opin. Struct. Biol.* **7,** 637–644
29. Coutinho, P. M., and Henrissat, B. (eds) (1999) in *Recent Advances in Carbohydrate Bioengineering* (Gilbert, H. J., Davies, G., Henrissat, B., and Svensson, B., eds) pp. 3–12, The Royal Society of Chemistry, Cambridge
30. Ong, E., Kilburn, D. G., Miller, R. C., Jr., and Warren, R. A. (1994) *J. Bacteriol.* **176,** 999–1008
31. Macleod, A. M., Gilkes, N. R., Escotecarlson, L., Warren, R. A. J., Kilburn, D. G., and Miller, R. C. (1992) *Gene* (*Amst.*) **121,** 143–147
32. Langsford, M. L., Gilkes, N. R., Singh, B., Moser, B., Miller, R. C., Warren, R. A. J., and Kilburn, D. G. (1987) *FEBS Lett.* **225,** 163–167
33. O'Neill, G. P., Anthony, R., Warren, J., Kilburn, D. G., and Miller, R. C. (1986) *Gene* (*Amst.*) **44,** 331–336
34. MacLeod, A. M., Lindhorst, T., Withers, S. G., and Warren, R. A. (1994) *Biochemistry* **33,** 6371–6376
35. Poon, D. K. Y., Ludwiczek, M. L., Schubert, M., Kwan, E. M., Withers, S. G., and McIntosh, L. P. (2006) *Biochemistry*, in press
36. Graham, R. W., Greenwood, J. M., Warren, R. A. J., Kilburn, D. G., and Trimbur, D. E. (1995) *Gene* (*Amst.*) **158,** 51–54
37. McLean, B. W., Bray, M. R., Boraston, A. B., Gilkes, N. R., Haynes, C. A., and Kilburn, D. G. (2000) *Protein Eng.* **13,** 801–809
38. Muchmore, D. C., McIntosh, L. P., Russell, C. B., Anderson, D. E., and Dahlquist, F. W. (1989) *Methods Enzymol.* **177,** 44–73
39. Delaglio, F., Grzesiek, S., Vuister, G. W., Zhu, G., Pfeifer, J., and Bax, A. (1995) *J. Biomol. NMR* **6,** 277–293
40. Goddard, T. D., and Kneeler, D. G. (1999) *SPARKY 3*, University of California, San Francisco
41. Hansen, M. R., Hanson, P., and Pardi, A. (2000) *Methods Enzymol.* **317,** 220–240
42. Clore, G. M., Gronenborn, A. M., and Bax, A. (1998) *J. Magn. Reson.* **133,** 216–221
43. Skrynnikov, N. R., and Kay, L. E. (2000) *J. Biomol. NMR* **18,** 239–252
44. Farrow, N. A., Muhandiram, R., Singer, A. U., Pascal, S. M., Kay, C. M., Gish, G., Shoelson, S. E., Pawson, T., Forman-Kay, J. D., and Kay, L. E. (1994) *Biochemistry* **33,** 5984–6003
45. Yang, D. W., and Kay, L. E. (1999) *J. Biomol. NMR.* **13,** 3–10
46. Dosset, P., Hus, J. C., Marion, D., and Blackledge, M. (2001) *J. Biomol. NMR.* **20,** 223–231
47. Daragan, V. A., and Mayo, K. H. (1997) *Prog. Nucl. Magn. Reson. Spectrosc.* **31,** 63–105
48. Braddock, D. T., Cai, M., Baber, J. L., Huang, Y., and Clore, G. M. (2001) *J. Am. Chem. Soc.* **123,** 8634–8635
49. Zweckstetter, M., and Bax, A. (2000) *J. Am. Chem. Soc.* **122,** 3791–3792
50. Kanelis, V., Donaldson, L., Muhandiram, D. R., Rotin, D., Forman-Kay, J. D., and Kay, L. E. (2000) *J. Biomol. NMR.* **16,** 253–259
51. Wishart, D. S., Bigam, C. G., Holm, A., Hodges, R. S., and Sykes, B. D. (1995) *J. Biomol. NMR.* **5,** 67–81
52. Kay, L. E., Torchia, D. A., and Bax, A. (1989) *Biochemistry* **28,** 8972–8979
53. Lipari, G., and Szabo, A. (1982) *J. Am. Chem. Soc.* **104,** 4546–4559
54. Tomme, P., Driver, D. P., Amandoron, E. A., Miller, R. C., Jr., Antony, R., Warren, J., and Kilburn, D. G. (1995) *J. Bacteriol.* **177,** 4356–4363
55. Ong, E., Gilkes, N. R., Miller, R. C., Warren, R. A. J., and Kilburn, D. G. (1993) *Biotechnol. Bioeng.* **42,** 401–409
56. Nikolova, P. V., Creagh, A. L., Duff, S. J. B., and Haynes, C. A. (1997) *Biochemistry* **36,** 1381–1388
57. Gerken, T. A., Butenhof, K. J., and Shogren, R. (1989) *Biochemistry* **28,** 5536–5543
58. Shogren, R., Gerken, T. A., and Jentoft, N. (1989) *Biochemistry* **28,** 5525–5536
59. Argos, P. (1990) *J. Mol. Biol.* **211,** 943–958
60. George, R. A., and Heringa, J. (2002) *Protein Eng.* **15,** 871–879
61. Bhandari, D. G., Levine, B. A., Trayer, I. P., and Yeadon, M. E. (1986) *Eur. J. Biochem.* **160,** 349–356
62. Radford, S. E., Laue, E. D., Perham, R. N., Martin, S. R., and Appella, E. (1989) *J. Biol. Chem.* **264,** 767–775
63. Williamson, M. P. (1994) *Biochem. J.* **297** 249–260
64. Creagh, A. L., Ong, E., Jervis, E., Kilburn, D. G., and Haynes, C. A. (1996) *Proc. Natl. Acad. Sci. U. S. A.* **93,** 12229–12234
65. Jervis, E. J., Haynes, C. A., and Kilburn, D. G. (1997) *J. Biol. Chem.* **272,** 24016–24023
66. Gilkes, N. R., Kilburn, D. G., Miller, R. C., Warren, R. A. J., Sugiyama, J., Chanzy, H., and Henrissat, B. (1993) *Int. J. Biol. Macromol.* **15,** 347–351